Journal of Applied Research and Technology

www.jart.icat.unam.mx

Journal of Applied Research and Technology 22 (2024) 243-250

Original

A non-intrusive wave measurement device for accurate analysis and real-time data

Z. M. Yusop[a]* • M. F. I. Y. Khan[b] • M. A. Jusoh[a] • A. Albani[a] • M. Z. Ibrahim[a] • M. S. Yahya[b] • M. H. M. Salleh[b]

[a]*Renewable Energy & Power Research Interest Group, Faculty of Ocean Engineering Technology, Universiti Malaysia Terengganu, 21030 Kuala Nerus, Terengganu, Malaysia*
[b]*Faculty of Ocean Engineering Technology, Universiti Malaysia Terengganu, 21030 Kuala Nerus, Terengganu, Malaysia*

Received 10 02 2023; accepted 01 24 2024
Available 04 30 2024

Abstract: This research aims to enhance our understanding of wave climate in ocean wave studies by creating a buoy-based system equipped with gyroscopes and accelerometers. This system allows for accurate measurement and analysis of ocean wave profiles, with primary objectives including the conversion of wave heave motion into electricity and forecasting wave strength for coastal erosion evaluations. The study's main goals encompass the development and integration of gyroscopes and accelerometers into the buoy system, the deployment of the device to collect wave profile data, and the analysis of this data using specialized software. The research culminated in the successful creation of a buoy capable of accurately measuring wave acceleration, velocity, and displacement with an approximate accuracy of 90%. This significant accomplishment advances ocean wave research and offers vital insights for sustainable coastal management, bolstering our grasp of wave climate and promoting informed decision-making and effective strategies to counter coastal erosion.

Keywords: Buoy, Wave acceleration, Velocity, Displacement, Ocean wave, Counter coastal erosion

*Corresponding author.
E-mail address: zulkifli.yusop@umt.edu.my (Z. M. Yusop).
Peer Review under the responsibility of Universidad Nacional Autónoma de México.

1. Introduction

Ocean waves, with their predictability, high energy density, and abundant source availability, offer significant potential as a renewable energy resource for generating electricity. In line with the global push for sustainable energy, the Malaysian government has set a target of 31% of the country's electricity to be generated from renewable energy (RE) sources by 2025 and 40% by the year 2035 (Sinar Harian and Bernama, 2021). Presently, solar photovoltaic technology dominates Malaysia's renewable energy sector, while oil, natural gas, coal, and hydropower form most of the country's energy mix, with some contributions from biomass and solar power as well (Abdullah et al., 2019). Despite having a considerable solar energy potential, Malaysia's current efforts fall short, with only 1 MW of solar capacity in place, while an estimated potential of more than 6500 MW remains untapped (Isa et al., 2010). As part of accelerating the transition to renewable energy, there is a need to explore alternative renewable sources. The country's vast 4,675 km coastline presents an untapped opportunity for harnessing wave energy through wave energy converter (WEC) technologies.

However, the development of WEC technologies faces challenges due to the incorrect collection of wave resources and the absence of in-situ wave data measurement (Ahn et al., 2021). Waves can be classified into seas, characterized by shorter periods, and swells, with longer periods and greater symmetry (Seenipandi et al., 2020). The variability of ocean wave resources presents a hindrance to the advancement of WEC technology, necessitating research into reliable real-time system control to optimize energy generation (Ringwood et al., 2023). This research focuses on three main objectives: first, the development of buoy-based devices equipped with measurement sensors for ocean wave profile assessment; second, data collection from the deployed buoy systems to record wave acceleration and direction; and third, the analysis of collected wave data using computational software, particularly MATLAB. The study employs theoretical research, modeling, simulation, and experimental evaluation.

One of the most critical aspects of ocean waves is their height, which relates to their energy content and destructive force. Understanding wave climate requires long-term observations, which presents a significant challenge in ocean wave research. Additionally, the location of interest for wave profile research is often in remote, fisherman-inhabited areas, complicating data collection (Laignel et al., 2023). Moreover, sensor technology limitations restrict data collection to deep waters, limiting measurement capability in shallow coastal regions (Skålvik et al., 2023).

To address these challenges, sensors must be installed on buoy systems floating freely on the ocean's surface. Achieving the research goals involves developing a floating buoy equipped with embedded measurement sensors for wave profile assessment, recording wave data related to acceleration and direction, and employing computational software analysis to derive valuable wave data results. By addressing these objectives, this research aims to contribute to the effective harnessing of ocean wave energy, advancing the development of WEC technologies, and enhancing Malaysia's sustainable coastal management strategies and achieving its renewable energy goals.

2. Methodology

There are three methods that were emphasized in achieving the objectives that were highlighted. First is device fabrication, where for this step, it is crucial to do it very carefully so that the floating device which is buoy use does not have any issues. The device that was set up by using hardware is a buoy that can function to flow in the ocean after deploying it and recording data.

2.1. Device fabrication

The buoy's main body has a diameter of 4 inches and a total height of 4 ft. It is enclosed with endcaps on both ends to protect the measurement sensor inside the polyvinyl chloride (PVC) pipe from water damage. Additionally, a smaller PVC pipe, 3 inches in diameter and 2 ft in height, filled with weight, serves as ballast, allowing the buoy to partially sink in the ocean and maintain a vertical orientation. Four red-marked floats, depicted in Figure 1, are evenly attached around the buoy's rounded body at its partially upright height. These floats move up and down in response to wave crests and troughs. Inside the top endcap of the device, the measurement sensors, comprising an accelerometer and gyroscope, are integrated with a microcontroller and rechargeable battery, enabling data recording for approximately 6 hours.

Figure 1. The complete measurement buoy is shown on the left, and the on-site measurement in the ocean is on the right.

2.2. Sensor calibration

In this research, the measurement sensor, depicted in Figure 2, is integrated with a 9-axis digital angle sensor. This sensor comprises an accelerometer, gyroscope, and an MPU9250 magnetometer. It is connected to a Cortex-M0 core processor, which houses a dynamic fusion algorithm and a Kalman filter. These ensure stable data output, excellent bias stability, a low noise level, and accurate measurements. The data transmission rate peaks at 200 Hz, which is ample for measuring a complete wave height cycle that occurs between 4 to 8 Hz. The electronic system is powered by a rechargeable lithium-ion polymer battery with a capacity of 250 mAh at 3.7 V. In this research, the device demonstrated the capability to operate continuously for close to 6 hours.

A pivotal aspect of this research is sensor calibration. It is imperative to calibrate the sensor meticulously to minimize errors. A challenge arises in converting the sensor's native output from acceleration form (ms^{-2}) to displacement form (cm). As illustrated in Figure 2, the sensor was positioned vertically at the starting point, adjacent to a standard ruler used as a reference for height. The measurement device was then manually raised to a 10 cm position and lowered back to its original position over several cycles. The recorded data, combined with a series of mathematical equations, was used to convert the readings into a height or displacement response. This conversion is crucial for verifying the calibration's accuracy. All simulations were conducted post-data processing using MATLAB software. If the graphed results in MATLAB do not match the actual height, it indicates an issue with the sensor or an error in the simulation code, necessitating further troubleshooting.

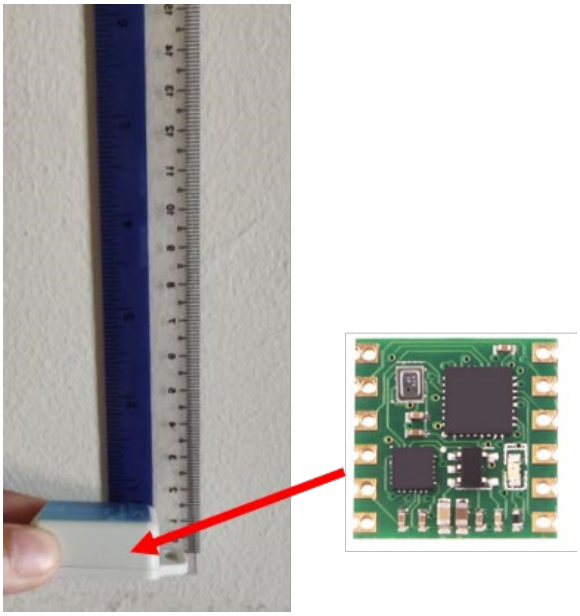

Figure 2. Measurement device and calibration procedure.

2.3. Data measurement

For the data collection phase, the buoy was deployed in the ocean for several hours to ensure a sufficient dataset was recorded, allowing for precise monitoring and analysis of the results. Several locations were evaluated for buoy deployment. The selected site was the shoreline area near the Universiti Malaysia Terengganu (UMT) campus, located at coordinates 5.4162317, 103.0894583, as depicted in Figure 3. The water depth at this location is approximately 3 meters, which is adequate to ensure the buoy remains vertically afloat and experiences wave heave motion. During the deployment period, the wave conditions were calm and not very turbulent.

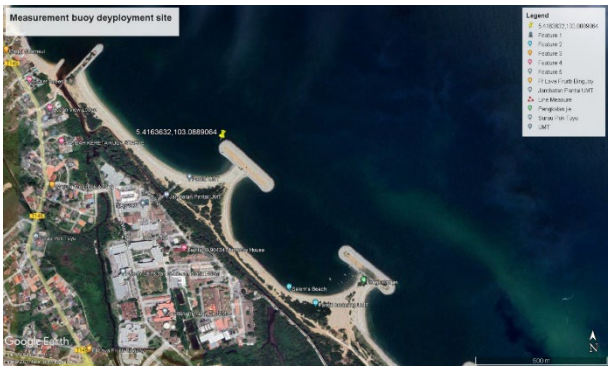

Figure 3. The location of the buoy has been deployed.

2.4. Data analysis

As mentioned earlier, the challenge in the data analysis is to interpret the sets of acceleration form (ms^{-2}) and transform it to displacement (cm) which is considered as a wave height or displacement in this research. The acceleration data (a_v) need to be twice integrated to determine the displacement (D_z) and shown as in Equation 1.

$$D_z = \iint a_v(t)dt \tag{1}$$

For sure to determine the accurate result is not so easy as that. The combination of multiple data recorded by multiple kinds of sensors needs to be first extracted. The raw data needs to be properly analyzed and only specific categories of data will be used from the overall recorded data. These required data categories including time (t), roll angle (φ), pitch angle (θ), yaw angle (ψ) and the measured accelerations in the X, Y, and Z directions (X_s,Y_s,Z_s) will be selected based on reference from mathematical equations.

There are various electronic correction schemes developed for wave height monitoring buoys that incorporate an acceleration sensor. Bender introduced five methods for wave height calculation using a 6-axis motion sensor, which measures both acceleration and angular velocity (Bender et al., 2010). These methods calculate buoy displacement based on

the non-gravitational acceleration along the z-axis (A_Z) in the earth-oriented coordinate system. A rotation matrix is applied to convert the acceleration values from the sensor's coordinate system (X_e, Y_e, Z_e) to the earth's coordinate system, from which the A_Z values are then derived (Minami et al., 2020).

$$[X_e] = [a_1 \quad b_1 \quad c_1][X_s] \tag{2}$$

$$[Y_e] = [a_2 \quad b_2 \quad c_2][Y_s] \tag{3}$$

$$[Z_e] = [a_3 \quad b_3 \quad c_3][Z_s] \tag{4}$$

Where the values of *a, b,* and *c* are defined as follows:

$$a_1 = \cos\theta \cos\psi \tag{5}$$

$$b_1 = \sin\phi \sin\theta \cos\psi - \cos\phi \sin\psi \tag{6}$$

$$c_1 = \cos\phi \sin\theta \cos\psi + \sin\phi \sin\psi \tag{7}$$

$$a_2 = \cos\theta \sin\psi \tag{8}$$

$$b_2 = \sin\phi \sin\theta \sin\psi + \cos\phi \cos\psi \tag{9}$$

$$c_2 = \cos\phi \sin\theta \sin\psi - \sin\phi \cos\psi \tag{10}$$

$$a_3 = -\sin\theta \tag{11}$$

$$b_3 = \sin\phi \cos\theta \tag{12}$$

$$c_3 = \cos\phi \cos\theta . \tag{13}$$

To accurately calculate the vertical displacement of the accelerometer, it is crucial to separate and exclude the gravitational acceleration component (g) from the recorded measurements. Where g is the gravity constant (9.81 ms^{-2}). The desired A_Z value, corresponding to the vertical acceleration component, is obtained using Equation 14.

$$A_z = g(1 - Z_e) = g[1 - (a_3X_s + b_3Y_s + c_3Z_s)] \tag{14}$$

After calculating the A_Z value, the vertical displacement can be determined by performing double integration including one more data point from the recorded raw data, which is time *(t)* in seconds. The calculated vertical displacement of the buoy represents the wave height or displacement. For accurate calculation of A_Z, it is essential to actual record the data for the roll, pitch, and yaw angles from the gyroscope sensor. These angles are necessary to perform the conversion of acceleration values from the sensor coordinate system to the earth coordinate system, which enables accurate calculation of A_Z. Within the MATLAB software, custom source code has been developed and adjusted to follow the equations stated in Equations 1 until 14. The code includes the conversion from acceleration into velocity and subsequently into displacement.

3. Result and analysis

3.1. Calibration analysis

The sensor was calibrated during the device fabrication stage. As depicted in Figure 4, the acceleration graph was plotted against a time series after calculating the AZ value in MATLAB. The graph indicates that the peak acceleration ranges from 20 ms^{-2} to 25 ms^{-2} throughout 300 s. The graph's pattern is irregular because, during calibration, the sensor was manually lifted and down without a consistent speed reference. Even slight changes in movement speed and tilting while holding the sensor can affect the recorded data. However, this irregularity mirrors real-world wave conditions, where wave height and occurrence are uneven and do not follow a uniform pattern.

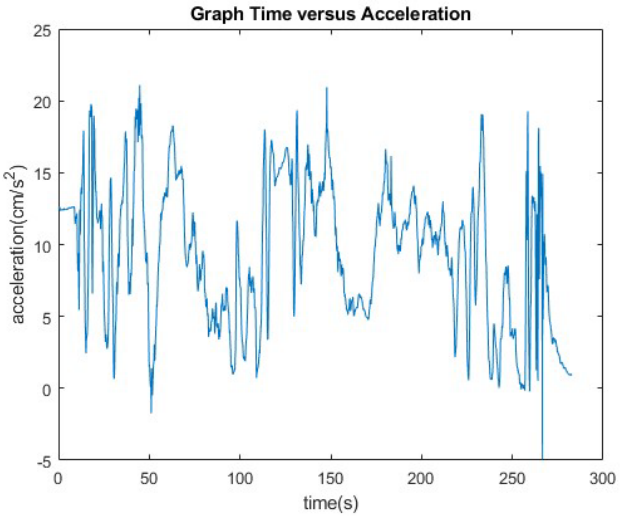

Figure 4. Acceleration graph response (A_Z) for calibration.

Figure 5 shows the MATLAB coding that is used to find the A_Z which is the non-gravitational acceleration from the data recorded by the measurement sensor.

Figure 6 shows the coding in MATLAB to find the velocity by performing one-time integration for the value of A_Z that was obtained previously.

In Figure 7, the graph of velocity shows that a sloped line, whether ascending or descending, indicates a change in velocity. The steeper the slope, the greater the rate of velocity change. The area under the velocity versus time graph, specifically within a 300 s interval, represents the object's displacement or distance covered during that period. The size

of this area gives insight into the total displacement of the waves. Reversals in the graph's slope signify changes in the direction of motion. For example, a shift from positive to negative velocity, or the reverse, indicates a change in direction, as seen between 50 s and 250 s. A horizontal line on the graph would represent a constant velocity, but such a pattern is absent in this graph. A line with zero slope indicates no change in velocity over time, signifying a constant speed. Therefore, the graph does not show any periods of constant velocity. The highest peak of the graph reaches approximately 13.5 ms^{-1}, while the lowest is around -1 ms^{-1}. This lowest peak closely aligns with the actual height at which the setup was established.

In Figure 8, MATLAB coding is presented to find the final parameter which is displacement and from the coding also can observe that the response of the displacement data has been directly converted into a graph form as depicted in Figure 9.

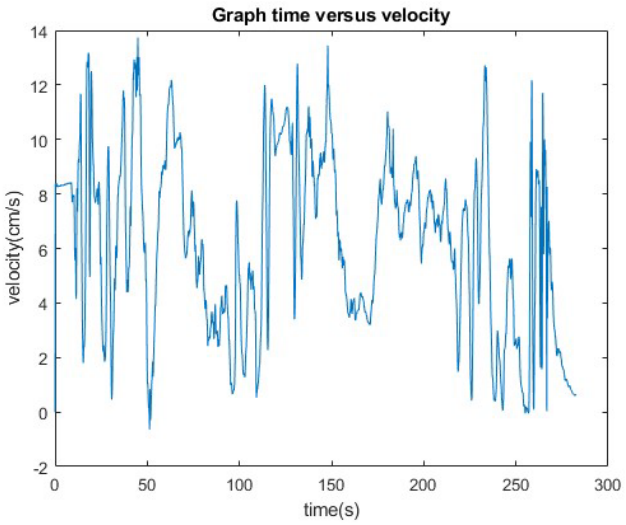

Figure 7. Velocity graph interpreted from acceleration A_Z

```
% Load data from table
%CALIBRATION PART
data = readtable (DCN. 'xlsx');
% set paramet that want to use from the data
T = data.(1); %time
double s;
R_a = data.(9)  ; %roll angle = angle x
P_a = data.(10) ; %pitch angle= angle y
X_s = data.(3)  ; %acceleration x
Y_s = data.(4)  ; %acceleration y
Z_s = data.(5)  ; %acceleration z
g = 9.81 ;        %value of gravity

for i = 1:1693
    a3 = -sin(P_a) ;
    b3 = sin(R_a).*(cos(P_a)) ;
    c3 = cos(R_a).*(cos(P_a)) ;
    Ze = (a3.*X_s)+(b3.*Y_s)+(c3.*Z_s) ;
    Az = g.*(1-Ze) ;
end

figure
plot(T,Az) ;
```

Figure 5. MATLAB code to measure A_Z from recorded data.

```
for i = 1:1693
    v(i+1,1)=0.5.*Az(i)+Az(i+1)*(T(i+1)-T(i)) ;
end
figure
plot(T,v);
data.v =v;
```

Figure 6. MATLAB code to determine the velocity from A_Z

```
for i = 1:1693
    d(i+1,1)=0.5.*v(i)+v(i+1)*(T(i+1)-T(i)) ;
end
figure
plot(T,d);
data.d =d;
```

Figure 8. MATLAB code to determine the displacement from velocity.

Figure 9 displays a displacement response with a peak close to 9 cm. When compared to the height measured during the calibration process, this result is deemed successful. The response from the displacement graph and the reference height are closely aligned, with an estimated error of ~10%. Thus, there is not a significant difference between the actual height and the height shown in Figure 9. It is important to note that the height in this calibration is measured in centimeters (cm). The displacement graph in Figure 9 can be further analyzed alongside velocity and acceleration graphs for a holistic understanding of the sensor's motion. Differentiating the displacement graph yields the velocity graph, and differentiating the velocity graph produces the acceleration graph. This analytical approach offers deep insights into the dynamics of the sensor's movement. Additionally, the area between the displacement graph and the time axis within a specific interval in Figure 9 represents the total displacement of the buoy during that time. The size of this area indicates the overall distance covered, which can be equated to the wave's height.

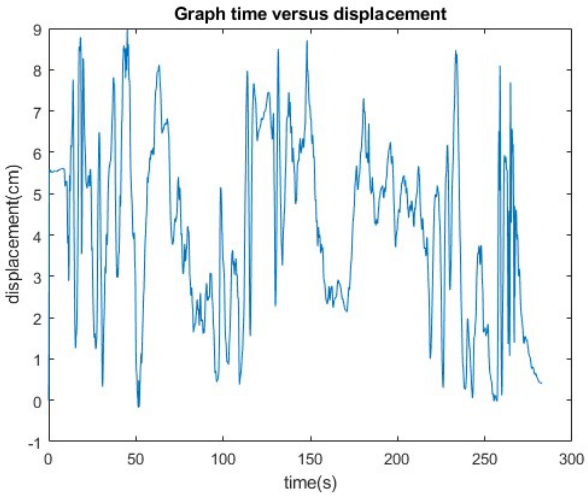

Figure 9. Displacement graph interpreted from velocity.

3.2. Experimental analysis

The raw data or the data that were collected in the ocean also has its result that has been analyzed and elaborated in the form of acceleration graph, velocity graph, and displacement graph.

3.2.1. Acceleration

Figure 10 illustrates transitions between different states of acceleration. A notable change is evident where the acceleration abruptly shifts from positive to negative, indicating a few instances of transition from acceleration to deceleration. The obtained acceleration values are presented as a graph against time, providing a clear view of how both the direction and magnitude of acceleration change. In this graph, a positive slope signifies positive acceleration. Lower values correspond to periods of constant or minimal acceleration, while peaks or spikes indicate moments of instantaneous acceleration. To achieve the results shown in Figure 10, raw data was processed and converted into the A_Z value. This conversion allows us to derive the A_Z values essential for further research, such as determining the displacement or height of ocean waves. The MATLAB code used to calculate the A_Z value, as depicted in Figure 5, was employed.

3.2.2. Velocity

Figure 11 shows the graph for the velocity that obtained after executed the MATLAB code similarly as shown in Figure 6. The direction of velocity is determined by the slope of the graph and in general a positive slope corresponds to positive velocity, while a negative slope indicates negative velocity or movement in the opposite direction. From the analysis, the average peak of wave velocity upon conducting the measurement is around 10 ms^{-1}.

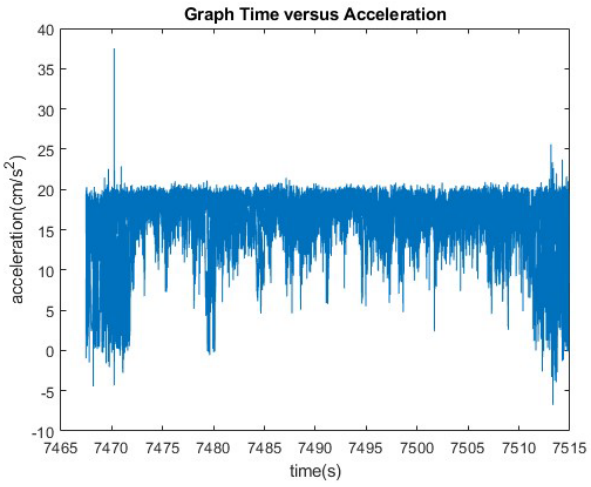

Figure 10. Acceleration graph response (A_Z) for actual wave measurement.

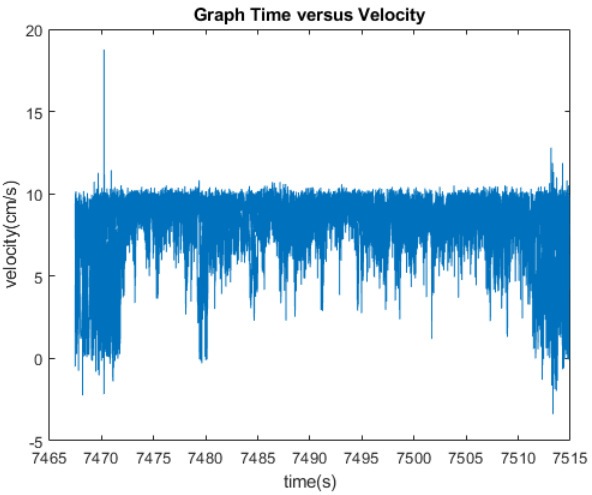

Figure 11. Velocity graph for the measured ocean wave.

3.2.3. Displacement

From this research work, the result is indicated in the displacement graph where it is the result obtained by performing a double integration value of A_Z. To determine the wave displacement, the integration process from velocity into displacement is required by using the MATLAB code given in Figure 8. The displacement measured in centimeters (cm), can be defined as the height of the ocean wave. Obtaining this measurement enhances our understanding of wave climate, facilitating informed decision-making and the development of

effective solutions to combat coastal erosion. The results for the ocean wave height at the proposed location, UMT beach, are presented in Figure 12.

As depicted in Figure 12, the recorded ocean wave heights are low, with an average peak height reaching around 5 cm. This is likely because the data was collected in mid-April 2023, after the monsoon season, which typically ends around February each year. During the monsoon season, ocean waves and turbulent waves are notably intense, contributing significantly to coastal erosion.

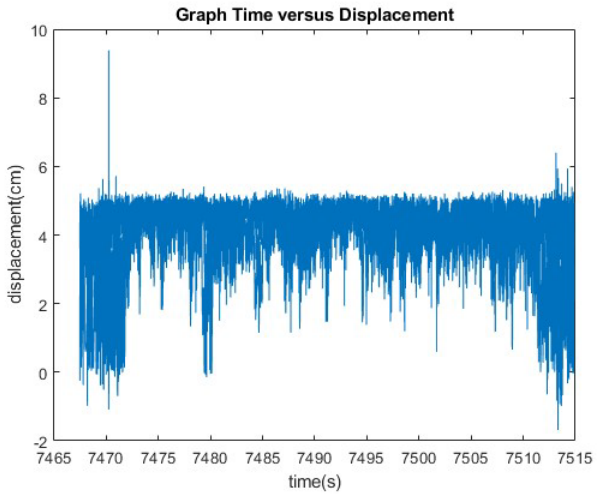

Figure 12. Displacement of the ocean waves.

4. Conclusions

This research work delves into the practical implications of maritime operations, offering valuable insights to professionals such as sailors and fishermen. The precise data on wave height, acceleration, and ocean depth derived from this research can significantly enhance their safety measures and navigation efficiency. Furthermore, the study holds substantial commercial promise. It paves the way for nations to tap into ocean wave energy as a renewable source of electricity. The wave profiles captured in this research could be instrumental in wave heave motion technology, facilitating the conversion of wave energy into electricity. This potential application could play a pivotal role in propelling renewable energy initiatives and promoting sustainable development goals. In addition, wave profile measurements play a crucial role in assessing the viability of installing floating photovoltaic solar panels offshore by providing critical data on wave height, frequency, and direction, which are essential for ensuring the structural stability and energy efficiency of solar installations in dynamic wave surfaces.

In wrapping up, the research has made remarkable progress in comprehending wave climate through the creation of a buoy-based system that integrates gyroscopes and accelerometers. The system's capacity to accurately measure and analyze ocean wave profiles has broadened the scope for electricity generation from wave heave motion and wave strength prediction for coastal erosion assessments. The successful creation of this device, capable of measuring wave acceleration, velocity, and displacement with precision, has not only propelled ocean wave research forward but also offered critical insights for sustainable coastal management strategies. This research has enriched our understanding of wave climate, thereby fostering informed decision-making and the formulation of effective solutions to counter coastal erosion.

Conflict of interest

The authors have no conflict of interest to declare.

Funding

This research was supported in part by UMT/TAPE-RG-2023/55451, whose generous funding made it possible to conduct this research and achieve valuable insights.

References

Abdullah, W. S. W., Osman, M., Ab Kadir, M. Z. A., & Verayiah, R. (2019). The potential and status of renewable energy development in Malaysia. *Energies*, *12*(12), 2437. https://doi.org/10.3390/en12122437

Ahn, S., Neary, V. S., Allahdadi, M. N., & He, R. (2021). Nearshore wave energy resource characterization along the East Coast of the United States. *Renewable Energy*, *172*, 1212-1224. https://doi.org/10.1016/j.renene.2021.03.037

Bender, L. C., Guinasso, N. L., Walpert, J. N., & Howden, S. D. (2010). A comparison of methods for determining significant wave heights—Applied to a 3-m discus buoy during Hurricane Katrina. *Journal of atmospheric and oceanic technology*, *27*(6), 1012-1028. https://doi.org/10.1175/2010JTECHO724.1

Laignel, B., Vignudelli, S., Almar, R., Becker, M., Bentamy, A., Benveniste, J., ... & Verpoorter, C. (2023). Observation of the coastal areas, estuaries and deltas from space. *Surveys in Geophysics*, *44*(5), 1309-1356. https://doi.org/10.1007/s10712-022-09757-6

Isa, A. M., Magori, H., Niimura, T., & Yokoyama, R. (2010). Multi-criteria generation optimal mix planning for Malaysia's additional capacity. International Journal of Energy and Environment, 4(4), 221-228.

Ringwood, J. V., Zhan, S., & Faedo, N. (2023). Empowering wave energy with control technology: Possibilities and pitfalls. *Annual Reviews in Control*. https://doi.org/10.1016/j.arcontrol.2023.04.004

Skålvik, A. M., Saetre, C., Frøysa, K.-E., Bjørk, R., & Tengberg, A. (2023). Challenges, limitations, and measurement strategies to ensure data quality in deep-sea sensors. *Frontiers in Marine Science*, 10. https://doi.org/10.3389/fmars.2023.1152236

Seenipandi, K., Ramachandran, K. K., & Kumar, P. (2021). Ocean remote sensing for spatiotemporal variability of wave energy density and littoral current velocity in the Southern Indian offshore. In *Remote Sensing of Ocean and Coastal Environments* (pp. 47-63). Elsevier. https://doi.org/10.1016/B978-0-12-819604-5.00004-4

Malaysia kongsi rancangan peralihan tenaga dengan Menteri Tenaga ASEAN. (2021, June 22). Astro Awani Network Sdn Bhd. https://www.sinarharian.com.my/article/145599

Minami, Y., Idoue, A., & Utsunomiya, E. (2020). Wave Height Measurement Systems Extended a Personal Ocean Observation Buoy. In *Global Oceans 2020: Singapore–US Gulf Coast* (pp. 1-6). IEEE. https://doi.org/10.1109/IEEECONF38699.2020.9389014